Enhancing Landsat Data Acquired Under Very Low Illumination

John M. Miller and *Greta J. Burger*
Northern Remote Sensing Laboratory, Geophysical Institute, University of Alaska, Fairbanks, AK 99775-0800

ABSTRACT: We have examined the potential utility of MSS images with sun elevation-angles between minus 4° and plus 10° during the winters of 1984-85 and 1985-86 using Landsat-4 and -5 data acquired by the Alaskan Quick-Look system. When band 1 and band 2 sensors have been switched to the high-gain mode, we show that it is possible to delineate open leads in sea ice with a sun angle of minus 4° by stretching the 0 to 4 range of digital numbers to the full contrast of a photographic image. Land features can be imaged down to 0°, showing (snow covered) forests or brush contrasted with barren tundra. Dune deposits on the order of 20 feet in height are visible, and snow cover and ice characteristics on large lakes can be determined. We conclude that one should not discount the value of Landsat data acquired with solar angles below 10°. Some natural features actually are enhanced by low incident-angles of illumination.

INTRODUCTION

FOR FIVE MONTHS of the year, the University of Alaska's Landsat Quick-Look program customarily deals with MSS data acquired under conditions of relatively low illumination. Figure 1 (after NASA/USGS) is a chart depicting solar elevation-angles at the mid-morning overpass for Landsat by month throughout the year and as a function of local latitude. The non-symmetrical expression of the elevation contours is a result of the inclination of the Earth's axis relative to the sun, combined with the consistent timing of daily Landsat events. It is not intuitively obvious, but the Landsat orbital parameters, which support universal mid-morning passes, also happen to favor higher solar angles in the northern hemisphere compared to the southern hemisphere.

The graph shows that the solar elevation is below 10° for about four and one-half winter months at 70° north latitude—the approximate location of Alaska's North Slope. (The southern hemisphere case is much worse. Solar angles at 70°S are below 10° for six and one-quarter months per year, at the mid-morning passes of Landsat.)

Normally, Landsat data would not be acquired along the northern coast of Alaska from 15 October through 1 March, if the minimum of a 10° solar angle is used as a guideline. Owing to the critical interest in exploration and extractive activities, as well as navigation and research interests in the behavior of sea ice, there was motivation to challenge the assumption that Landsat images with low illumination were of questionable value.

The Quick-Look system of the University of Alaska receives a direct downlink of the real-time MSS signal from NOAA's command and data acquisition station in Fairbanks. The raw data are stored on-the-fly onto a bank of magnetic disks. The data can be processed and enhanced into full-resolution images within an hour or two of the satellite overpass (Miller, 1981).

We respond to customer requests for routine coverage of sea-ice, among other things, which inherently involves data acquired with low illumination (George, 1983). The challenges of generating useful images from low sun-angle data have led us to re-examine some basic assumptions about Landsat data acquisition and image enhancement.

During the winter season we ask NOAA to switch the MSS sensors to the high-gain (X3) mode to compensate for lower terrestrial irradiance. Bands 1 and 2 (visible wavelengths) are affected by the higher gain, but bands 3 and 4 (reflective infrared), which lack the capability of selectable gain settings, are not affected.

We examined data from a winter pass and tabulated the brightest pixels that appeared in a swath that extended from the sunlight terminator (Row 12) to land's end (Row 23). We used high-gain MSS data from Path 79 on 23 November 1984 to define the digital number (DN) maxima found in the raw data. The maximum values of Row 12 data and of Row 23 data are compared in Table 1.

It should be noted that band 4 saturates less quickly at low sun angles because this detector is a silicon photodiode that is less sensitive than the photomultipliers of the other bands. Band 4 has about twice the dynamic range of the other infrared channel, band 3 (NASA/USGS, 1979). For this reason, the effects of wavelength-dependent Rayleigh scattering are masked on the band 4 data, unless one accounts for the response characteristics inherent in

PHOTOGRAMMETRIC ENGINEERING AND REMOTE SENSING,
Vol. 52, No. 6, June 1986, pp. 801–807.

0099-1112/86/5206-801$02.25/0

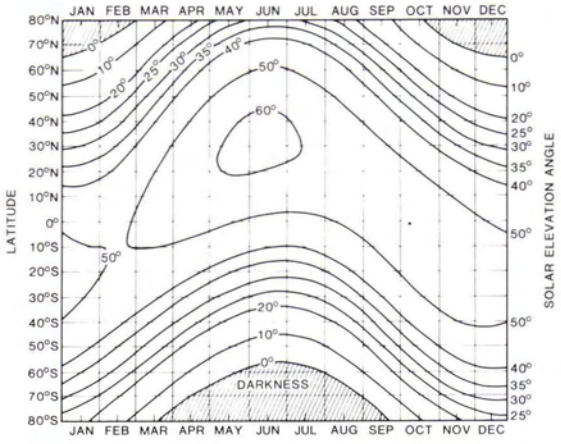

FIG. 1. Graph of solar elevation angle at various latitudes. The elevation angle "contours" apply to mid-morning Landsat passes for each month of a calendar year. The cross-hatched areas on the graph represent dark conditions when the sun is below the horizon at the time of Landsat overflights.

TABLE 1. NORMALIZED HIGH-GAIN BRIGHTNESS EXTREMES

	Band	0° Elev Max White	Normalized ×1	13° Elev Max White	Normalized ×1
1	Grn ×3	20	7	200	67
2	Red ×3	100	33	240	80
3	IR1 ×1	85	85	220	220
4	IR2 ×1	50	100*	160	320*

*The maximum DN were multiplied by a factor of two to obtain the normalized values for Band 4.

this detector. For purposes of comparison with the other bands, the band 4 DN values were doubled for Table 1.

The scene contents throughout this path varied from snow-covered mountains and forested valleys to clouds and open water over the North Pacific Ocean. Several conclusions may be drawn:

- Bands 1 and 2 probably will not reach saturation, defined in our system as 255 DN, on south-facing, snowy landscapes unless the solar elevation-angle is between 15° to 20°. Thus, it is advantageous to use the high-gain mode of the satellite for all passes where the sun elevation angle would be 20° or less.
- Band 2 (red) in the high-gain mode will show the greatest contrast when the scene is illuminated by very low sun angles. Band 2 is twice as bright under such conditions as is band 4 (IR2), which is the usual high-contrast band of choice with normal illumination. Our tests showed that band 2 is consistently a better choice than band 4 for sun angles less than about 5°.
- If IR wavelengths are needed to discriminate open water from new ice, band 3 is vastly superior to band 4 for low sun angles. Band 3 consistently provided better contrast with low illumination than did band 4.
- Not surprisingly, there is a strong red dominance in the data from visible wavelengths at extremely low elevations of the sun. The reddishness is caused by increased Rayleigh scattering of the shorter wavelengths during the greatly lengthened path of solar radiation through the atmosphere. Similar dominance by the shorter IR wavelengths is evident when one factors out the X3 gain applied to bands 1 and 2.

IMAGE ENHANCEMENT TECHNIQUES

If we generate an image directly from the raw values of MSS data, the result likely would be quite disappointing. A photographic print has the inherent limitations of portraying only 16 shades of gray between maximum black and maximum white. MSS data, after being stretched in dynamic range by the image formatter, have 256 potential values of brightness between black (0 DN) and white (255 DN).

Typical MSS data tend to occupy far less than the full range of values between 0 and 255. Depending upon the exact ground cover, the range of values may vary. For example, forested valley floors may vary between 30 and 90 DN. The data in subscenes are usually concentrated in rather narrow ranges of DN. Sea ice that lacks open-water leads is an example of data whose values may populate a narrow DN range, perhaps extending from 70 to 90.

Displaying MSS data with a narrow dynamic range would create a thin, washed-out image that was useless. There are 256 potential brightness levels in MSS data, which means that each shade of gray on the print would have to represent 16 brightness levels of the data, if we choose to linearly map the image from zero for black to 255 for white.

A contrast-stretch enhancement can exaggerate the small variations in brightness of the raw data so that the image becomes easier to interpret. A contrast stretch is generated by mapping each discrete gray-level encountered in the image, on a pixel-by-pixel basis, into a modified output value according to a pre-selected algorithm. The maximum and minimum gray-levels of the input are separated, or stretched, as far apart as possible (without undue black or white saturation) so as to completely fill the dynamic range of the output print. The linear contrast-stretch algorithm is defined by

$$Y_{ij} = 255[(X_{ij} - \text{Min})/(\text{Max-Min})] \qquad (1)$$

As a general rule, the more narrow the range of brightnesses in the subscene of interest, the more severe the contrast stretch should be. A ×4 ratio is considered a minor stretch for key features of average contrast. In some instances we get better results with a contrast stretch approaching ×20.

RESULTS

Figure 2 is a sequence of three adjacent frames, all taken from Path 66 acquired 31 January 1985,

open-leads, and newly frozen leads in the ice of the eastern Beaufort Sea. Included are Rows 8, 9, and 10 of an area approximately 200 km west of Banks Island and just north of Mackenzie Bay in Canada. The elevation angle of the sun was 0, +1, and +2 degrees, and the solar azimuth was 170, 168, and 166 degrees, respectively.

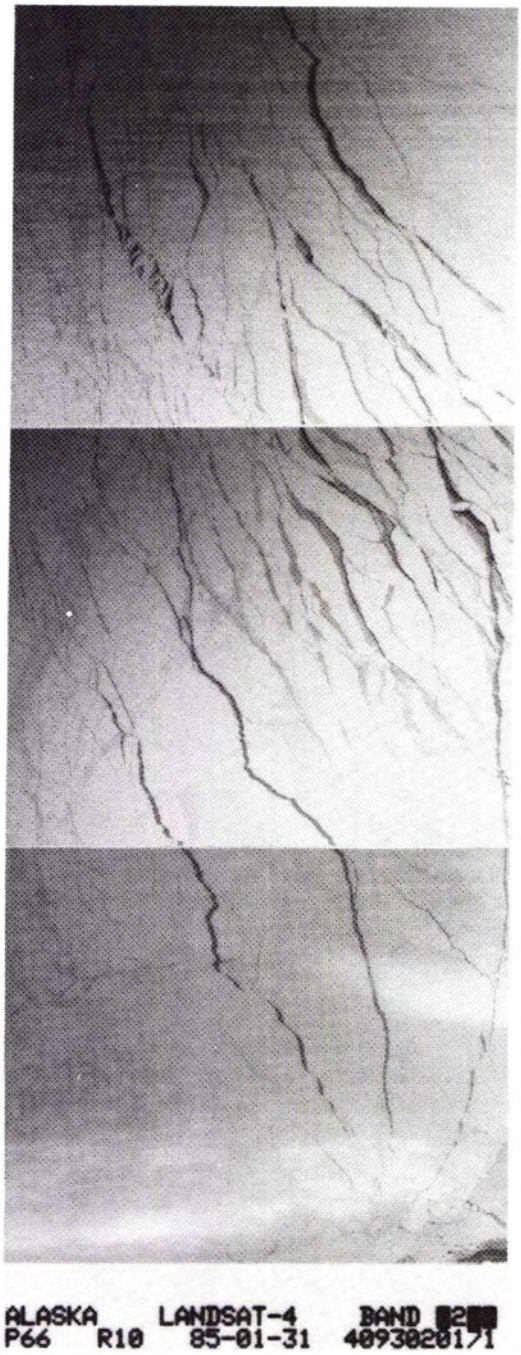

FIG. 2. Three adjacent Landsat frames from 31 January 1985. Sea-ice details are prominent with low solar elevation angles of 0, +1, and +2 degrees, respectively.

The effects of the solar azimuth are highly visible in these images when one compares the brightness of the lower right with the upper left portion of each frame. The sunlight-terminator line extends diagonally, with a descending left-slope, at about the center of the junction of Rows 8 and 9. The ice features above the terminator are illuminated only by scattered sunlight.

Differing enhancements were applied to these scenes in order to compensate for the changing level of irradiance from frame to frame. Although linear contrast-stretching was used throughout, the white thresholds were set higher for each succeeding frame, as follows:

The top scene has a white threshold set to 25 (i.e., 25 DN is set to maximum white 255 DN). This is a $\times 10$ contrast stretch. Saturation in the image, caused by our processing, starts to occur only at the lower right corner; however, the MSS sensors themselves were not being saturated. Substantial coherent noise is also apparent on the data.

The middle scene has a white threshold set to 40, and clearly shows ice details adjacent to the saturated appearance of the ice-pack in the scene above. This enhancement is an example of a contrast stretch of 6.4 times. A slight amount of coherent noise is evident.

The bottom scene has a white threshold set to 70, and again picks up the ice details starting to be lost to saturation at the lower right of the previous frame. This is an example of a $\times 3.6$ contrast stretch. The entire scene is sunlit and the terminator line is no longer evident. Some clouds have saturated in the image, but the ice features have not. As is frequently the case with solar angles near zero, the shadows from these clouds are not visible because no shadows are cast onto the Earth's surface.

Figure 3 is Row 11 from Path 67, one day earlier than Figure 2. Figure 3 has an illumination of 3° and was generated by a $\times 3$ contrast stretch. The white threshold was adjusted so that the cloud-related brightness on the right (Mackenzie Bay) and the southeast-facing slopes of the British Mountains (lower left center) were somewhat saturated. Subtle terrain relief is materially enhanced by this low solar angle. The exact coastal boundary is evident although the gently tapering landfall is covered by landfast ice and snow. The terrain relief of Herschel Island, center, is clearly apparent on the original print.

Figure 4 consists of a strip of four adjacent frames from Path 77 acquired 28 January 1985 and shows ice details in the western Beaufort Sea when the sun was below the horizon. Rows 7 through 10 are included in the strip, with landfall occurring at Harrison Bay, Alaska, on Row 10. Solar elevation angles were −3, −2, −1, and +1 degrees, respectively, starting at the top frame.

Linear enhancements were used for all four frames. The white thresholds were set individually as fol-

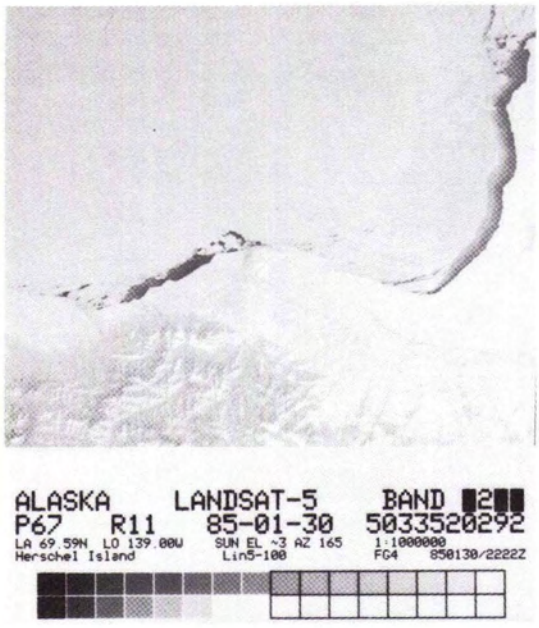

FIG. 3. Ice features in Canada's Mackenzie Bay, coastal boundaries, and terrain relief are evident in this scene. These data were acquired 30 January 1985, one day earlier than the data of Figure 2. The solar angle was +3 degrees.

lows:

The 1st (top) frame, Row 7, with a −3° solar angle, was generated by setting the white threshold at 10 DN. This enhancement is a severe ×25 contrast stretch that was selected to emphasize the information that largely was buried in the sensor noise. Only the most broad outline of fracture patterns and polynyas (open-water leads) are visible, owing to the low prevailing irradiance.

The coherent noise of the MSS sensors here shows up as a "wood-grain" pattern, which is typical of homogeneous scenes from Landsat-4, and to a lesser extent from Landsat-5. System noise is present on all channels of MSS data of Landsat-4 and -5 (Rice, 1983; Likens, 1983; Kiefer, 1983; Alford, 1983; Markham, 1983). Our observations show that system noise on Landsat-5 MSS tends less toward the wood-grain pattern and more toward a "stitching" pattern. The system noise usually is not visible in images from either satellite that are generated from data acquired with normal illumination. The high-contrast features of normal data mask the noise and subdue its visibility below the threshold of recognition in image interpretation.

The 2nd frame, Row 8, with a −2° solar angle, was generated by setting the white threshold at 15 DN. This is a ×17 contrast stretch. About the same amount of ice detail is visible as in the frame above. The increasing brightness toward the lower right corner reflects the increasing irradiance caused by atmospheric scattering. No direct sunlight reaches the ice surface on this scene. The system noise is still very evident.

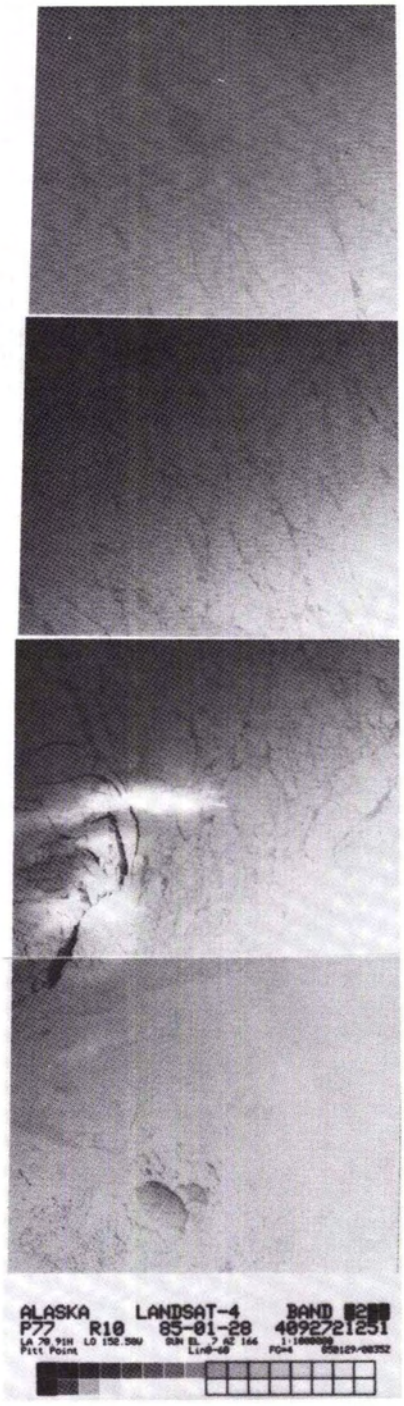

FIG. 4. Four adjacent Landsat frames showing ice details in the western Beaufort Sea, with the sun actually below the horizon, on 28 January 1985. Solar angles were −3, −2, −1, and 0 degrees, respectively.

The 3rd frame, Row 9, with a −1° solar angle, was generated by setting the white threshold to 50

DN. This is a $\times 5$ contrast stretch, and much more detail can be seen in the sea ice. In addition to polynyas and fracture patterns, one can see that the larger floes may contain multi-year ice. This frame includes another example of apparently "shadowless" clouds.

The 4th (bottom) frame, Row 10, with a $+0.7°$ solar angle, was generated by setting the white threshold to 60 DN, which is only a slight change from the enhancement of the preceding frame. Open water, the zone of rubble ice (which typically forms between the moving ice-pack and the landfast ice along shorelines), the land-fast ice, and coastal lakes and landforms are shown in remarkably useful detail—all this information is gleaned from data acquired with the sun at the horizon.

Of particular interest is the recognition of Pik Dunes, the gentle dunes (visible on the master copy of the image) along the bottom of the frame slightly to the right of center. These undulating dunes are sparsely vegetated and have crests averaging only 20 feet in height, and they weave between the pattern of wind-aligned lakes. It is interesting to note that the dunes elongate parallel to the prevailing winds, but the thaw lakes align themselves orthogonally to the wind direction.

The dunes are examples of subtle terrain-features that are visible only in Landsat images with very low solar angles; their topographic relief is too slight to appear in USGS contour maps.

Figure 5 consists of four adjacent frames from Path 81 along the northwest coast of Alaska, covering the region from Point Barrow (top frame) to Kotzebue Sound (bottom frame). Included in the strip are Frames 9 through 12 from 2 December 1985.

Starting at the top, the solar angles were -4, -3, -2, and -1 degrees, respectively. The contrast-stretch enhancements used were very severe, from $\times 85$ for the two topmost frames to $\times 51$ for the bottom frame. Good detail is evident in the landfast ice and broken floes in the topmost frames, even though the sun was below the horizon.

Figure 6 also reveals details of complex shear motion of the ice off the northern coast of Siberia. This sequence is from Path 93, Rows 10 - 12, from 6 December 1985, and shows images with solar angles of -4, -3 and $-2°$, respectively. Wrangel Island appears in the top frame, and the northeastern coast of the U.S.S.R. in the middle frame.

Figure 7 is Path 68, Row 17, from 13 November 1985, shows detailed circulation patterns in Cook Inlet, the city of Anchorage (center) and surrounding terrain. The extensive bright fields in the upper left constitute the major agricultural development at Point MacKenzie. Of particular interest are the patterns of floating ice which trace the major currents in the estuary. The concentration of ice near Fire Island (dark object, left center) is near a shoal that threatens navigation in the shipping channel to the Port of Anchorage.

FIG. 5. A strip of Landsat images covering the region from the northwest coast of Alaska (Point Barrow at the top) to the DeLong Mountains. These frames show landfast ice and sea-ice features illuminated by solar angles of -4 degrees (top) to -1 degree (bottom) on 2 December 1985.

CONCLUSIONS

To ensure a good dynamic range for the sensor outputs, and to minimize shadows in terrain with

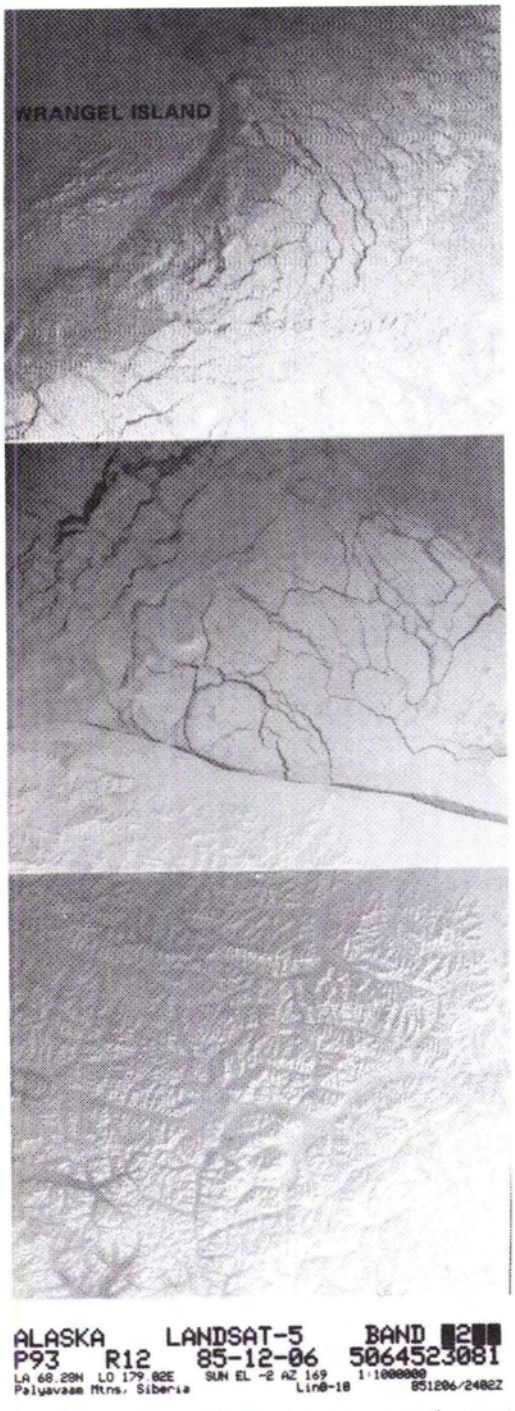

FIG. 6. Three adjacent Landsat frames over the western Chukchi Sea on 6 December 1985. Ice conditions are visible off Wrangel Island (upper frame) and the northeast coast of Siberia (middle frame) when the sun was 4-degrees below the horizon.

FIG. 7. A single Landsat frame of Cook Inlet and Anchorage with surrounding terrain obtained on 13 November 1985. The ice in the estuaries traces the circulation patterns that prevail during receding tides. The concentration of ice near Fire Island, the dark object in left center, marks the confluence of currents near the location of shoals, which are a risk to navigation.

moderate to high relief, Landsat data customarily are acquired when the sun elevation-angle is ten degrees or greater. Limiting the data acquisition in this fashion produces a mid-winter period from two to four months when there are no Landsat data available in extreme northern latitudes (NASA/USGS, 1979).

The winter hiatus is even more pronounced in the southern hemisphere, because there Landsat passes inherently occur earlier in the local day. By acquiring MSS data with solar angles as low as 0°, it is possible to add a total of eight weeks to the spring and fall observing seasons, in both the northern and southern hemispheres.

We have examined the utility of MSS images with sun elevation angles between minus 4° and plus 10° during the winter of 1984-85 using Landsat-4 and -5 data acquired by the Alaskan Quick-Look system. We designed particularly severe contrast-enhancements for processing the digital data and found that some applications can be supported with solar angles as low as minus 4°.

We believe that it is possible to determine the presence or absence of open leads in sea ice with a sun angle of minus 3° by stretching the 0 to 7 range of digital numbers to the full contrast of a photographic image. Land features can be usefully imaged down to 0°, showing (snow covered) forests

or brush contrasted with barren tundra. Dune deposits on the order of 20 feet in height are visible, and snow cover and ice characteristics on large lakes can be inferred. Some natural features actually are enhanced by low incident-angles of illumination.

REFERENCES

Alford, W.L., and M.L. Imhoff, 1983. Radiometric Accuracy Assessment of Landsat-4 Multispectral Scanner (MSS) Data. *Proc. Landsat-4 Early Results Symposium*, Vol.II, NASA, pp. 69–72.

George, T.H., J.M. Miller, and J. Zender-Romick, 1983. The First Year of Operation of the Alaskan Landsat Quick-Look System. *Proc. Seventeenth International Symposium on Remote Sensing of Environment*, Vol.III, pp. 1253–1262.

Kiefer, H.H., E.M. Eliason, and P.S. Chavez, Jr., 1983. Intraband Radiometric Performance of the Landsat 4 Thematic Mapper. *Proc: Landsat-4 Science Characterization Early Results Symposium*, VOL.III, pp. 471–495.

Likens, W.C., and R.C. Wrigley, 1983. Impact of Landsat MSS Sensor Differences on Change Detection Analysis. *Proc. Landsat-4 Science Characterization Early Results Symposium*, Vol.I, NASA, 159–175.

Markham, B.L., and J.L. Barker, 1983. Spectral Characterization of the Landsat-4 MSS Sensors. *Proc. Landsat-4 Early Results Symposium*, Vol.II, NASA, 73-80.

Miller, J.M., N. Campbell, and R. Mackinnon, 1981. An Experimental Landsat Quick-Look System for Alaska. *Proc. Seventh International Symposium on Machine Processing of Remotely Sensed Data*, pp. 639–646.

NASA/USGS, 1979. *Landsat Data Users Handbook* (revised edition). Sioux Falls, SD.

Rice, D.P., and W.A. Malila, 1983. Investigation of Radiometric Properties of Landsat-4 MSS. *Proc. Landsat-4 Science Characterization Early Results Symposium*, Vol.I, NASA, 57-76.

(Received and accepted 3 March 1986)